

Induction of $\alpha 1$ and $\alpha 2$ gene expression in selective immunoglobulin A deficiency

HIROKO SUZUKI, HIDEO KANEKO, JIN RONG, NORIO KAWAMOTO, TSUTOMU ASANO, EIKO MATSUI, KIMIKO KASAHARA, TOSHIYUKI FUKAO and NAOMI KONDO

Department of Pediatrics, Graduate School of Medicine, Gifu University, Gifu, Japan

Received December 3, 2007; Accepted January 24, 2008

Abstract. Immunoglobulin A deficiency (IgAD) is the most common immunodeficiency, but the pathogenesis of most cases of IgAD is poorly understood. The gene and protein expression levels of members of the IgA subclasses in IgAD patients were analyzed by a reverse transcriptase (RT)-PCR method that could differentiate between $\alpha 1$ and $\alpha 2$ gene expression. Three selective, 5 partial and 2 secondary IgAD patients were examined. Peripheral blood mononuclear cells which were unstimulated or stimulated with TGF- $\beta 1$ and PMA for 24 h were cultured. The IgA1/IgA2 expression ratios were measured by zone densitometry. Three bands appeared (the $\alpha 1$ and $\alpha 2$ genes and a hetero-duplex formation), owing to the difference of 39 bases between $\alpha 1$ and $\alpha 2$ mRNAs. In the controls, there were no significant differences in the IgA1/IgA2 ratios between unstimulated and stimulated cells. In selective IgAD patients, both $\alpha 1$ and $\alpha 2$ gene expression was induced following stimulation, and $\alpha 1$ gene expression was induced more dominantly than in the other IgAD patients following stimulation. Based on our results, suppression of $\alpha 1$ gene expression may be related to the pathogenesis of IgAD.

Introduction

Human immunoglobulin A (IgA) is the major type of secreted antibody consisting of two subclasses, IgA1 and IgA2. The ratios of IgA1/IgA2 in secretions vary, and the functions of IgA1 and IgA2 in immune response remain unclear (1,2).

IgA deficiency (IgAD) is the most common immunodeficiency. The prevalence in Caucasians is approximately 1 in 500, while the prevalence in the Japanese is much lower; approximately 1 in 18,000 (3-5). IgAD is associated with a variety of infections, allergies, autoimmune disorders, gastro-

intestinal diseases, malignancies, endocrinopathies, neurological diseases and genetic disorders (3,6). IgAD is often associated with other forms of immunoglobulin deficiencies, including IgG subclasses and IgE deficiency (7-10). Certain IgAD patients have an α gene deletion, but the pathogenesis of some cases of IgAD is still poorly understood. Recently, it has become clear that certain common variable immunodeficiency and IgAD patients possess mutations in TNFRSF13B [encoding TACI (transmembrane activator and calcium-modulator and cyclophilin ligand interactor)] (11). The class switch disorder in IgA-producing B lymphocytes is one of the most important factors in IgAD patients (12). Asano *et al* (13) suggested that the decreased expression level of Ia germline transcripts before a class switch might be the cause of selective IgAD, and that B-cell differentiation might be disturbed after a class switch in partial IgAD patients. Husain *et al* (14) reported that the increased destruction of a subset of B cells is a cause of the inability of IgAD patients to produce IgA. Many studies have reported that certain cytokines, such as IL-4, IL-10, anti-CD40 and TGF- β , play important roles in the production of IgA (15,16).

The molecular weights of the IgA heavy chain of the $\alpha 1$ and $\alpha 2$ genes are approximately 53 kD each, and the α -chain constant region is encoded by three exons: Ca1, Ca2 and Ca3. Ca2 includes a hinge region at its 5'-end. The hinge region of the $\alpha 2$ gene has a deletion of 13 amino acids compared with that of the $\alpha 1$ gene (1,17). The genes encoding $\alpha 1$ and $\alpha 2$ resemble each other closely and, in IgAD patients in particular, it has been difficult to make a quantitative analysis. In order to elucidate the pathogenesis of, and immunological reaction to, IgAD, we analyzed the gene expression of the IgA subclasses in IgAD patients. In this study, we devised a semiquantitative method in order to determine the gene expression levels of members of the IgA subclasses, and analyzed selective, partial and secondary IgAD patients. Using this method, the gene expression of the IgA subclasses could be analyzed in detail.

Materials and methods

Subjects. As shown in Table I, we analyzed three selective IgAD patients (nos. 1, 2 and 3) with serum IgA levels below the detection limit (<5 mg/dl), five partial IgAD patients (nos. 4, 5, 6, 7 and 8) with serum IgA levels >5 mg/dl but -2 standard deviations below the normal levels, and two

Correspondence to: Dr Hiroko Suzuki, Department of Pediatrics, Graduate School of Medicine, Gifu University, 1-1 Yanagido, Gifu 501-1194, Japan

E-mail: hori_hiro2002@yahoo.co.jp

Key words: immunoglobulin A deficiency, immunoglobulin A subclasses, IgA1/IgA2 gene expression ratios, TGF- $\beta 1$

Table I. Immunological data of patients.

Patient no.	Gender	Age (years)	Serum level (mg/dl)			IgG subclass (mg/dl)			
			IgG	IgA	IgM	IgG1	IgG2	IgG3	IgG4
Selective IgA deficiency									
1	M	10	1363	<5	146	619	255.0	57.3	33.9
2	F	11	1640	<5	117	949	400.0	47.7	90.2
3	F	17	1261	<5	137	630	625.0	35.1	18.4
Partial IgA deficiency									
4	M	4	1223	17	120	933	<8.0	22.8	<3.0
5	F	3	1644	15	150	878	47.9	17.3	32.1
6	F	3	869	27	106	306	69.3	27.6	3.8
7	M	4	887	45	101	295	97.0	40.0	4.4
8	M	4	1624	8	100	1090	120.0	74.7	<3.0
Secondary IgA deficiency									
9	F	7	913	12	105	602	148.0	52.8	16.5
10	M	13	705	9	39	852	345.0	49.8	6.4

secondary IgAD patients (nos. 9 and 10) whose condition was caused by epileptic medication. Ten controls were also included in this study. We obtained informed consent from the patients, controls or their parents.

Cell preparation and culture. Peripheral blood mononuclear cells (PBMCs) were collected in heparin and separated by gradient centrifugation in Ficoll-Paque (Amersham Bioscience, Uppsala, Sweden) (18). Cells were suspended at a density of 10^6 /ml and cultured for 24 h in an RPMI-1640 medium supplemented with 10% heat-inactivated fetal calf serum, 2 mmol/l L-glutamine, 100 U/ml penicillin and 100 μ g/ml streptomycin. Some of the PBMCs were stimulated with phorbol myristate acetate (PMA) (10 ng/ml) (Sigma Aldrich, St. Louis, MO, USA) and recombinant human TGF- β 1 (1 ng/ml) (R&D Systems, Inc., Wiesbaden, Germany) for 24 h.

cDNA synthesis and PCR amplification. We extracted total RNA from PBMCs using an Isogen kit (Nippon Gene, Tokyo, Japan), and cDNA synthesis was carried out using 2 μ g of total RNA with oligo-dT and M-MLV reverse transcriptase (Invitrogen, Carlsbad, CA). We used the following PCR primers, both of which were designed against the common sequence area of the α 1 and α 2 genes: sense 5'-CCT GGT CAC CGT CTC CTC A-3' (within the J exon; Gene Bank accession no. L20778) and antisense 5'-TCA CGC TCA GGT GGT CCT TG-3' (within the C α CH2 exon) (19). The PCR fragments included the CH1, hinge and CH2 regions, and their sizes were 532 bp for the α 1 gene and 493 bp for the α 2 gene. The PCR program was 35 or 40 cycles of 94°C for 1 min, 60°C for 1 min, and 72°C for 1 min, using 1 or 2 μ l of cDNA as the template. The PCR products were run on 4% agarose gels for 120 min. Glyceraldehyde-3-phosphate dehydrogenase (GAPDH) was used as a control.

Zone densitometry analysis. The IgA1/IgA2 gene expression ratios in stimulated cells were measured using zone densitometry. The peaks of each of the three bands were detected and measured. Half of the intensity of the heterozygous band was added to each of the α 1 and α 2 band intensities, and then the IgA1/IgA2 ratios were calculated. Subcloning was conducted according to the following steps. After electrophoresis the bands, including the α 1 and α 2 genes, were cut out, and DNA extraction was performed. We transformed the DNA fragments into a T-vector, then cultured and picked up the colonies. The plasmid DNA was extracted and digested to completion with *EcoRI*. We distinguished two isotypes, α 1 and α 2 genes, by the sizes of DNA bands on the gels; some of the α 2 fragments were separated into two bands because one of the allotypes of the α 2 gene, the A2m(2) allotype, had an *EcoRI* site (20).

Quantification of IgA in plasma. IgA was measured using enzyme-linked immunosorbent assay (ELISA). ELISA plates were coated overnight at 4°C with goat anti-human IgA (Bethyl, Montgomery, TX), which was diluted to 1:100 with 0.05 M sodium carbonate, pH 9.6. After washing, the plates were incubated with standard serum and plasma dilutions. IgA was detected by horseradish peroxidase (HRP)-labeled goat anti-human IgA (Cappel, Organon Teknika, Turnhout, Belgium), which was diluted to 1:10,000 with 1% BSA, 50 mM Tris-HCl, pH 8.0, 0.15 M NaCl and 0.05% Tween-20. The samples were tested repeatedly. The lower limit of IgA detection was 5 ng/ml.

Quantification of IgA subclasses in plasma. The levels of the IgA subclasses in plasma were measured using ELISA. For IgA1, coating was performed using a mouse monoclonal anti-IgA1 antibody (NI69-11), and detection of IgA1 was

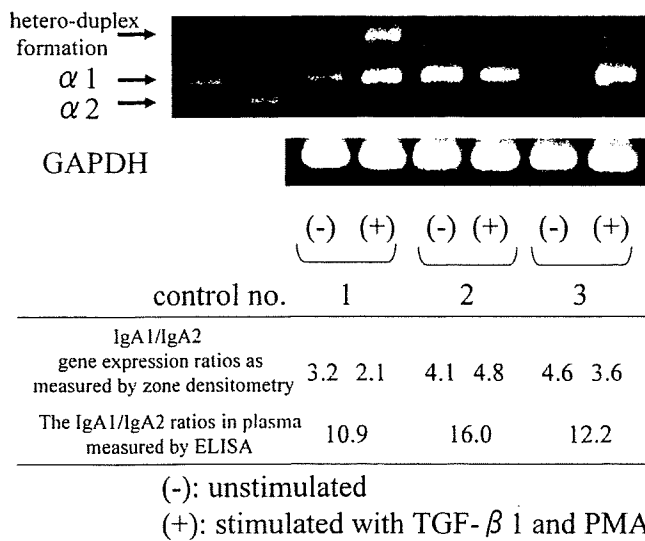


Figure 1. Expression of the $\alpha 1$ and $\alpha 2$ genes in healthy controls. PBMCs from three healthy controls were cultured for 24 h in the absence or presence of stimulation with TGF- β 1 and PMA. After PCR, three bands appeared representing $\alpha 2$ and $\alpha 1$ gene expression and hetero-duplex formation, as indicated by arrows. GAPDH was used as a control. The IgA1/IgA2 expression ratios following stimulation were measured by zone densitometry, and the IgA1/IgA2 ratios in plasma were measured using ELISA.

performed using an HRP-labeled goat anti-human IgA antibody (Cappel, Organon Teknika) (21). For IgA2, coating was performed with goat anti-human IgA, and detection of IgA2 was performed using a mouse anti-human IgA2-HRP antibody (B3506B4) (22). ELISA plates were coated overnight at 4°C with mouse monoclonal anti-IgA1 (diluted to 1:200 with PBS-0.02% Tween-20) or goat anti-human IgA (diluted to 1:100 with PBS-0.02% Tween-20). After washing, plates were incubated with standard serum and plasma dilutions. IgA1 was detected using goat anti-human IgA-HRP antibody

(diluted 1:10,000 with PBS-0.02% Tween-20), and IgA2 was detected using mouse anti-human IgA2-HRP antibody (diluted to 1:1000 with PBS-0.02% Tween-20). Samples were tested repeatedly. The lower limits of IgA1 and IgA2 detection were 5 and 1 μ g/ml, respectively.

Statistical analysis. Significant differences between two groups were analyzed by paired t-tests. The correlation coefficients were determined by Pearson's product-moment correlation coefficient. $p < 0.05$ was considered to be statistically significant.

Results

PCR amplification of $\alpha 1$ and $\alpha 2$ gene expression in control PBMCs. RT-PCR analysis was performed using primer pairs that amplified both $\alpha 1$ and $\alpha 2$ mRNAs and could distinguish between them owing to the deletion of 39 bases in the hinge region of the $\alpha 2$ mRNA. As shown in Fig. 1, the controls displayed an intense $\alpha 1$ band and a less intense, shorter $\alpha 2$ band in all three PCR conditions. Another band with less electrophoretic mobility than the $\alpha 1$ band was determined to be a hetero-duplex formation from the $\alpha 1$ and $\alpha 2$ fragments, because the subcloning of this band yielded clones of both $\alpha 1$ and $\alpha 2$ fragments. The expression of the $\alpha 1$ and $\alpha 2$ genes in the healthy controls is shown in Fig. 1. The gene expression of the PCR products tended to be enhanced more strongly when cells were stimulated with TGF- β 1 and PMA. In all of the healthy controls, $\alpha 1$ gene expression was dominant. The IgA1/IgA2 expression ratios were measured by zone densitometry in the healthy controls and were found to vary (1.1-4.8) among the controls. There were no significant differences in the IgA1/IgA2 expression ratios of unstimulated cells and cells stimulated with TGF- β 1/PMA ($p > 0.05$). To confirm the IgA1/IgA2 ratios as analyzed by zone densitometry, we counted the number of colonies from the PCR products. The

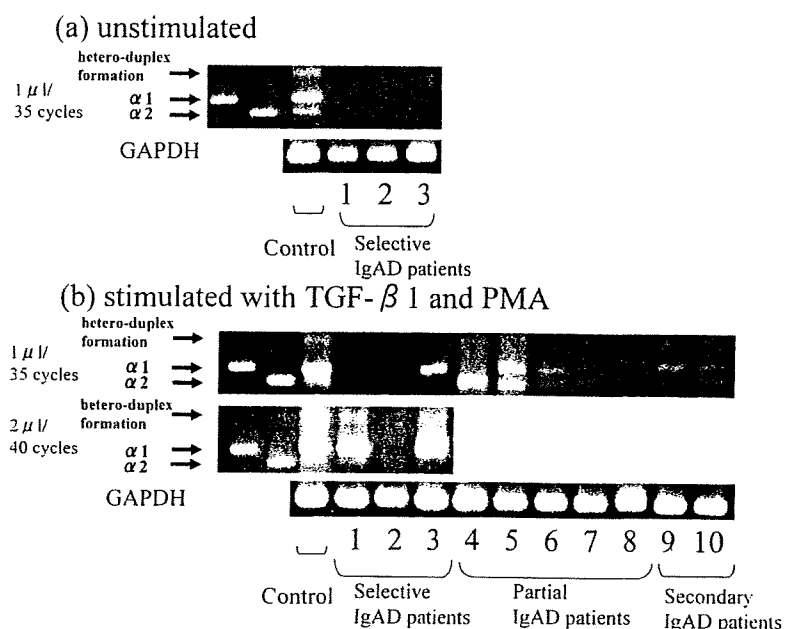


Figure 2. Expression of the $\alpha 1$ and $\alpha 2$ genes in IgAD patients. PBMCs from IgAD patients were cultured for 24 h in the absence (a) or presence (b) of stimulation with TGF- β 1 and PMA. In each case, 1 or 2 μ l of cDNA was used as a template and 35 or 40 cycles were run. GAPDH was used as a control.

number of colonies correlated with the IgA1/IgA2 ratios determined by zone densitometry (data not shown).

PCR amplification of $\alpha 1$ and $\alpha 2$ gene expression in IgAD patients. Expression of the $\alpha 1$ and $\alpha 2$ genes in the IgAD patients is shown in Fig. 2. Stimulation of cells with TGF- β 1/PMA induced expression of mature transcripts in some selective IgAD patients. No selective IgAD patients showed any bands without stimulation, while selective IgAD patients (nos. 1 and 3) showed two or three bands following stimulation. Some partial IgAD patients (nos. 5, 6 and 7) and secondary IgAD patients (nos. 9 and 10) showed $\alpha 2$, $\alpha 1$ and heteroduplex gene expression following stimulation, while patient no. 4 showed only $\alpha 2$ gene expression. This patient was found to have a deletion of $\alpha 1$, $\gamma 2$, $\gamma 4$ and ϵ genes, as in a previously reported case (10). Using this method, we identified the second case of $\alpha 1$ gene deletion in Japan. Partial IgAD patient no. 8 showed no bands using this RT-PCR method. The IgA1/IgA2 ratios of IgAD patients analyzed by zone densitometry are shown in Table II. ND (not detected) in Table II means that gene expression was not detected or that the peaks were too faint to detect when analyzed by zone densitometry. The expression levels of both the $\alpha 1$ and $\alpha 2$ genes relative to GAPDH expression in IgAD patients were suppressed when compared with the controls (data not shown). In selective IgAD patients, both $\alpha 1$ and $\alpha 2$ gene expression was induced following stimulation. In particular, $\alpha 1$ gene expression was more dominant than that of $\alpha 2$ in these patients when compared with the other IgAD patients and healthy controls.

IgA, IgA1 and IgA2 concentration in the controls and IgAD patients. The levels of IgA1 and IgA2 proteins in plasma are shown in Table III. ND (not detected) in Table III means that levels were below the detection limit. In all controls, the

Table II. IgA1/IgA2 gene expression ratios measured by zone densitometry.

Patient no.	IgA1/IgA2 gene ratios	
	Stimulation	
	(-)	TGF- β 1/PMA
Selective IgA deficiency		
1	ND	3.91 \pm 0.55
2	ND	ND
3	ND	7.04 \pm 1.22
Partial IgA deficiency		
4		No $\alpha 1$ gene transcripts
5		2.55 \pm 1.74
6		1.72 \pm 0.49
7		1.11 \pm 0.27
8		ND
Secondary IgA deficiency		
9		1.50 \pm 0.29
10		1.17 \pm 0.10
Controls (n=10)	2.56 \pm 1.22	2.35 \pm 1.20
ND, not detected.		

IgA1 levels in plasma were dominant. The IgA1/IgA2 gene expression ratios following stimulation measured by zone densitometry were strongly correlated with those of plasma levels measured using ELISA in the controls (n=10, r=0.917, t=6.53, p<0.05) (Fig. 1).

Table III. IgA subclass levels and the IgA1/IgA2 ratios in plasma as measured using ELISA.

Patient no.	Plasma IgA, IgA1 and IgA2 levels (mg/dl)			IgA1/IgA2 ratios
	IgA	IgA1	IgA2	
Selective IgA deficiency				
1	2.13 \pm 0.01	2.48 \pm 0.26	ND	NC
2	ND	ND	ND	NC
3	4.00 \pm 0.59	2.16 \pm 0.74	ND	NC
Partial IgA deficiency				
4	9.18 \pm 2.87	ND	13.7 \pm 1.39	NC
5	5.16 \pm 0.21	2.71 \pm 0.36	ND	NC
6	10.11 \pm 0.13	8.28 \pm 0.52	0.91 \pm 0.25	8.40
7	37.46 \pm 8.36	29.29 \pm 6.83	4.88 \pm 0.54	6.97
8	6.53 \pm 0.52	6.28 \pm 0.67	0.86 \pm 0.45	8.87
Secondary IgA deficiency				
9	11.23 \pm 1.91	8.59 \pm 1.77	1.17 \pm 0.36	6.56
10	0.54 \pm 0.06	0.56 \pm 0.09	0.18 \pm 0.03	3.03
Controls (n=10)	154.01 \pm 37.89	119.61 \pm 34.69	20.44 \pm 8.63	7.96 \pm 4.14

ND, not detected; NC, not calculated.

Discussion

The serum IgA subclass levels of IgAD patients, especially selective IgAD patients, are very difficult to measure using ELISA, so there have been few reports concerning them. The expression levels of the $\alpha 1$ and $\alpha 2$ genes in most IgAD patients are low, and there have been no reports concerning the levels of mature transcripts of the IgA subclasses in patients (23-26). Wang *et al* (27) concluded that the cause of IgAD is a defect in the transcriptional factors important for post-switch $C\alpha$ gene transcription or a lack of signals for activation of the $C\alpha$ gene in IgA-switched cells. According to Hummelshoj *et al* (16), $\alpha 1$ and $\alpha 2$ germline transcripts in IgAD patients were induced by the stimulation of certain types of cytokines, such as TGF- $\beta 1$ and IL-4. Such stimulation can lead to the induction of germline transcripts and mature transcripts in IgAD patients. In our report, using stimulation of cells with TGF- $\beta 1$ and PMA, we induced expression of both $\alpha 1$ and $\alpha 2$ transcripts in cells from IgAD patients and measured the IgA1/IgA2 ratios. In the healthy controls, there were no significant differences in the IgA1/IgA2 ratios with or without stimulation. In the IgAD patients, the gene expression levels of both IgA subclasses were suppressed. Expression of the $\alpha 1$ gene was induced more dominantly than that of the $\alpha 2$ gene following stimulation in selective IgAD patients. Kitani and Strober (28) reported that *Staphylococcus aureus*, Cowan I and TGF- $\beta 1$ induce mature $C\alpha 1$ transcripts, but do not induce $C\alpha 2$ mature transcripts. Based on our results, suppression of $\alpha 1$ gene expression may be involved in the pathogenesis of selective IgAD. However, there was a discrepancy in the IgA1/IgA2 ratios based on gene expression levels and those based on protein expression levels. This discrepancy might have been caused by post-transcriptional modifications leading to, for example, protein or mRNA stability. The other possibility is that the production of IgA protein might have been different in peripheral circulating IgA-switched B cells and locally accumulated IgA-switched B cells, such as mucosal tissue. Secreted and membrane-localized IgA can not be distinguished by this method, and we are now investigating methods for the separation of membrane and secretory transcripts in each IgA subclass.

Our method was effective for detecting mature transcripts of IgA subclasses in cases whose serum IgA levels were under the detection limit. Additional patient analysis is needed to clarify the mechanism of the pathogenesis of IgAD.

Acknowledgements

This study was supported in part by a grant from The Ministry of Health, Labor and Welfare of Japan.

References

1. Kerr MA: The structure and function of human IgA. *Biochem J* 271: 285-296, 1990.
2. Kazeeva TN and Shevelev AB: Unknown functions of immunoglobulin A. *Biochemistry* 72: 485-494, 2007.
3. Cunningham-Rundles C: Physiology of IgA and IgA deficiency. *J Clin Immunol* 21: 303-309, 2001.
4. Hammarstrom L, Vorechovsky I and Webster D: Selective IgA deficiency and common variable immunodeficiency. *Clin Exp Immunol* 120: 225-231, 2000.
5. Latiff AH and Kerr MA: The clinical significance of immunoglobulin A deficiency. *Ann Clin Biochem* 44: 131-139, 2007.
6. Schaffer FM, Monteiro RC, Volanakis JE and Cooper MD: IgA deficiency. *Immunodef Rev* 3: 15-44, 1991.
7. Bottaro A, De Marchi M, De Lange GG and Carbonara AO: Gene deletions in the human immunoglobulin heavy chain constant region gene cluster. *Exp Clin Immunogenet* 6: 55-59, 1989.
8. Lefranc MP, Hammarstrom L, Smith CI, *et al*: Gene deletions in the human immunoglobulin heavy chain constant region locus: molecular and immunological analysis. *Immunodef Rev* 2: 265-281, 1991.
9. Plebani A, Carbonara AO, Bottaro A, *et al*: Gene deletion as cause of associated deficiency of IgA1, IgG2, IgG4 and IgE. *Immunodef Rev* 4: 245-248, 1993.
10. Terada T, Kaneko H, Li AL, Kasahara K, Ibe M, Yokota S and Kondo N: Analysis of Ig subclass deficiency: first reported case of IgG2, IgG4, and IgA deficiency caused by deletion of $C\alpha 1$, $\psi C\gamma$, $C\gamma 2$, $C\gamma 4$ and $C\epsilon$ in a Mongoloid patient. *J Allergy Clin Immunol* 108: 602-606, 2001.
11. Castigli E, Wilson SA, Garibyan L, Rachid R, Bonilla F, Schneider L and Geha RS: TAC1 is mutant in common variable immunodeficiency and IgA deficiency. *Nat Genet* 37: 829-834, 2005.
12. Islam KB, Baskin B, Nilsson L, Hammarstrom L, Sideras P and Smith CI: Molecular analysis of IgA deficiency. *J Immunol* 152: 1442-1452, 1994.
13. Asano T, Kaneko H, Terada T, Kasahara Y, Fukao T, Kasahara K and Kondo N: Molecular analysis of B-cell differentiation in selective or partial IgA deficiency. *Clin Exp Immunol* 136: 284-290, 2004.
14. Husain Z, Holodick N, Day C, Szymanski I and Alper CA: Increased apoptosis of CD20⁺IgA⁺B cells is the basis for IgA deficiency: The molecular mechanism for correction *in vivo* by IL-10 and CD40L. *J Clin Immunol* 26: 113-125, 2006.
15. Marconi M, Plebani A, Avanzini MA, *et al*: IL-10 and IL-4 cooperate to normalize *in vivo* IgA production in IgA-deficient patients. *Clin Exp Immunol* 112: 528-532, 1998.
16. Hummelshoj L, Ryder LP, Nielsen LK, Nielsen CH and Poulsen LK: Class switch recombination in selective IgA-deficient subjects. *Clin Exp Immunol* 144: 458-466, 2006.
17. Koteswara R: Divergence of human α -chain constant region gene sequences. *J Immunol* 152: 5299-5304, 1994.
18. Kondo N, Fukutomi O, Agata H, *et al*: The role of T lymphocytes in patients with food-sensitive atopic dermatitis. *J Allergy Clin Immunol* 91: 658-668, 1993.
19. Klasen IS, Goertz JHC, van de Wiel GA, Weemaes CM, van der Meer JW and Drenth JP: Hyper-Immunoglobulin A in the hyperimmunoglobulinemia D syndrome. *Clin Diagn Lab Immunol* 8: 58-61, 2001.
20. Lefranc MP and Rabbits TH: Human immunoglobulin heavy chain A2 gene allotype determination by restriction fragment length polymorphism. *Nucleic Acids Res* 12: 1303-1311, 1984.
21. Camacho MT, Outschoorn I, Echevarria C, *et al*: Distribution of IgA subclass response to *Coxiella burnetii* in patients with acute and chronic Q fever. *Clin Immunol Immunopathol* 88: 80-83, 1998.
22. Beard LJ and Ferrante A: IgG4 deficiency in IgA-deficient patients. *Pediatr Infect Dis J* 8: 705-709, 1989.
23. Vlasselaer PV, Punnonen J and Vries JE: Transforming growth factor- β directs IgA switching in human B cells. *J Immunol* 148: 2062-2067, 1992.
24. Park SR, Kim HA, Chun SK, Park JB and Kim PH: Mechanisms underlying the effects of LPS and activation-induced cytidine deaminase on IgA isotype expression. *Mol Cells* 19: 445-451, 2005.
25. Islam KB, Nilsson L, Sideras P, Hammarstrom L and Smith CI: TGF beta-1 induces germ-line transcripts of both IgA subclasses in human B lymphocyte. *Int Immunol* 3: 1099-1106, 1991.
26. Nilsson L, Islam KB, Olafsson O, *et al*: Structure of TGF-beta 1-induced human immunoglobulin C alpha 1 and alpha 2 germ-line transcripts. *Int Immunol* 3: 1107-1115, 1991.
27. Wang Z, Yunis D, Irigoyen M, Kitchens B, Bottaro A, Alt FW and Alper CA: Discordance between IgA expression and the mRNA level in IgA-deficient patients. *Clin Immunol* 91: 263-270, 1999.
28. Kitani A and Strober W: Differential regulation of $C\alpha 1$ and $C\alpha 2$ germ-line and mature mRNA transcripts in human peripheral blood B cells. *J Immunol* 153: 1466-1477, 1994.



Brief report

Anaphylactoid transfusion reactions associated with a positively charged white-cell reduction filter: A case report

Michinori Funato *, Hideo Kaneko, Michio Ozeki, Kaori Kanda,
Toshiyuki Fukao, Naomi Kondo

Department of Pediatrics, Gifu University Graduate School of Medicine, Yanagido 1-1, Gifu 501-1194, Japan

Abstract

The effectiveness of a white-cell reduction filter to deplete contaminated leucocytes in preventing the harmful effects of transfusion is evident. However, several complications associated with a white-cell reduction filter have been identified. We report the first case of anaphylactoid reactions caused by a white-cell reduction filter with a positively charged surface. © 2008 Elsevier Ltd. All rights reserved.

1. Introduction

In 1990 Tielemans et al. described a life-threatening anaphylactoid reaction occurring within the very first minutes of hemodialysis using polyacrylonitrile (AN69) capillary dialyzers in three patients receiving angiotensin-converting enzyme (ACE) inhibitors [1]. In 1992 Olbricht et al. also described a similar anaphylactoid reaction due to low-density lipoprotein (LDL)-apheresis with dextran sulphate adsorption in patients receiving ACE inhibitors [2]. These anaphylactoid reactions were thought to be due to a bradykinin formation cascade, activated by using negatively charged white-cell reduction filters [3]. So far, several anaphylactoid reactions associated with white-cell reduction filters have been reported. However, anaphylactoid reactions associ-

ated with white-cell reduction filters having a positively charged surface have not been reported previously. Herein, we describe the first case of anaphylactoid reactions caused by a white-cell reduction filter with a positively charged surface in this paper.

2. Case report

A boy with recurrent anaplastic ependymoma of the brain was on chemotherapy at seven years of age. He had a pollen allergy. His father was Japanese and his mother was Filipino. At three years of age, he was found to have a brain tumor and received a complete surgical resection. At that time, he was not given a blood transfusion. Four years later, brain computed tomography (CT) showed a 6 × 5 cm mass lesion in the left frontal horn, which meant a recurrence of anaplastic ependymoma. He was subsequently treated by a total excision of the tumor. Postoperatively, he received radiation

* Corresponding author. Tel.: +81 58 2306386; fax: +81 58 2306387.

E-mail address: mfunato@mac.com (M. Funato).

therapy (a total of 30 Gy), stereotactic radiosurgery (SRS) (a total of 12 Gy) and four courses of multi-agent chemotherapy consisting of vincristine, etoposide, cyclophosphamide and cisplatin.

He required some transfusions of red blood cells, platelets and fresh frozen plasma for the side effects of bone marrow suppression during the treatment (Table 1). There was no trouble during the first and second transfusions of packed red blood cells and fresh frozen plasma, respectively. However, after starting infusion of leukocyte-poor red cells, which were filtered with a positively charged white-cell reduction filter (Sepacell RZ-2 filter, Asahi Med, Japan), as a third transfusion, he immediately developed a skin rash of the trunk, hypotension, blurred eyesight and unconsciousness. No stridor or dyspnea was observed. The transfusion was stopped and he was rescued by fluid resuscitation, epinephrine and hydrocortisone. We thought his reaction was allergic, associated with the transfusion. In the next infusion, washed red blood cells were used and nothing happened. In the fifth transfusion, we gave him prophylactic antihistamines and infused leukocyte-poor red cells, and similar anaphylactoid symptoms occurred immediately. His symptoms were resolved in several minutes by medical treatment. Subsequent transfusions of washed red blood cells or a platelet concentration were done without any problem.

3. Discussion

A transfusion of allogeneic cellular blood products is associated occasionally with adverse reactions and other complications, including febrile nonhemolytic transfusion reactions (FNHTR), graft-versus-host disease (GVHD), and immunomodulation and transmission of infectious agents, despite careful

donor selection and extensive testing [4]. The use of a white-cell reduction filter to deplete contaminated leucocytes is effective in reducing those harmful effects of transfusion, particularly alloimmunization and cytomegalovirus infection [5]. However, several complications associated with a white-cell reduction filter have been described. Herein, we have reported a rare case of anaphylactoid reactions associated with a white-cell reduction filter having a positively charged surface in a 7-year-old boy.

We thought his symptoms were caused by something related to the positive charge on the membrane. The leukocyte-poor red cells were made from washed red blood cells by passing them through a positively charged white-cell reduction filter at The Japan Red Cross. This patient only developed anaphylactoid symptoms twice when the former but not the latter was transfused. In addition, his clinical symptoms were very similar to anaphylactoid reactions during transfusion associated with a negatively charged white-cell reduction filter, which was reported in previous literature [6]. The possibility of other causes is unlikely, because his antibodies against HLA, IgA, haptoglobin, C4, C9, ceruloplasmin, and anti-alpha-2-microglobulin were all negative when examined at The Japan Red Cross Central Blood Center. In addition, this patient had a mild increase in his peripheral eosinophil count ($0.603 \times 10^9/L$) for allergic constitution and normal immunoglobulin G, A, M and E concentrations (1149 mg/dl, 175 mg/dl, 178 mg/dl and 150 IU/L, respectively).

Iwama examined the effect of temperature on bradykinin generation during the use of white-cell reduction filters. In this assay, a positively charged filter did not generate bradykinin at any temperature. However, a negatively charged one generated a lot of bradykinin when warm blood (37 °C) was

Table 1
All courses of transfusion in this patient during the treatment

No.	Blood product	Anaphylactoid reaction	A positively white-cell reduction filter	Prophylactic agent
1	Packed red blood cells	–	–	–
2	Fresh frozen plasma	–	–	–
3	Leukocyte-poor red cells	+	+	–
4	Washed red blood cells	–	–	–
5	Leukocyte-poor red cells	+	+	+
6	Platelet concentration	–	–	+
7	Washed red blood cells	–	–	+
8	Washed red blood cells	–	–	+
9	Washed red blood cells	–	–	+
10	Platelet concentration	–	–	+
11	Washed red blood cells	–	–	+

used but did not when cool blood (4 °C) was used [7]. In our patient, The Japan Red Cross prepared leukocyte-poor red cells at 4 °C and kept them at 4 °C. Then a blood transfusion was done at room temperature. Hence, bradykinin was not likely to cause any symptoms in our patient.

This case of anaphylactoid transfusion reactions associated with a positively charged white-cell reduction filter may be attributed to the fact that such reactions are not related to the charge on the membrane, but to a hypersensitivity reaction against something made by filtration through a white-cell reduction filter. In this respect, further work needs to be undertaken on the exact molecular nature of this reaction.

Acknowledgements

This study was supported in part by the Health and Labor Science Research Grants of the Research on Allergic disease and Immunology from the Ministry of Health, Labor and Welfare.

References

- [1] Tielemans C, Madhoun P, Lenaers M, Schandene L, Goldman M, Vanherweghem JL. Anaphylactoid reactions during hemodialysis on AN69 membranes in patients receiving ACE inhibitors. *Kidney Int* 1990;38:982–4.
- [2] Olbricht CJ, Schaumann D, Fischer D. Anaphylactoid reactions, LDL apheresis with dextran sulphate, and ACE inhibitors. *Lancet* 1992;340:908–9.
- [3] Takahashi TA, Abe H, Hosoda M, Nakai K, Sekiguchi S. Bradykinin generation during filtration of platelet concentrates with a white cell-reduction filter. *Transfusion* 1995;35:967.
- [4] Bordin JO, Heddle NM, Blajchman MA. Biologic effects of leukocytes present in transfused cellular blood products. *Blood* 1994;84:1703–21.
- [5] de Graan-Hentzen YCE, Gratama JW, Mudde GC, Verdonck LF, Houbiers JGA, Brand A, et al. Prevention of primary cytomegalovirus infection in patients with hematologic malignancies by intensive white cell depletion of blood products. *Transfusion* 1989;29:757–60.
- [6] Sano H, Koga Y, Hamasaki K, Furuyama H, Itami N. Anaphylaxis associated with white-cell reduction filter. *Lancet* 1996;347:1053.
- [7] Iwama H. Bradykinin-associated reactions in white cell-reduction filter. *J Crit Care* 2001;16:74–81.

Positioning of autoimmune TCR-Ob.2F3 and TCR-Ob.3D1 on the MBP85–99/HLA-DR2 complex

Zenichiro Kato^{†‡§¶||}, Joel N. H. Stern[†], Hironori K. Nakamura[§], Kazuo Kuwata[§], Naomi Kondo^{‡§¶||}, and Jack L. Strominger[†]

[†]Department of Molecular and Cellular Biology, Harvard University, Cambridge, MA 02138; and [‡]Department of Pediatrics, Graduate School of Medicine, [§]Center for Emerging Infectious Diseases, and [¶]Center for Advanced Drug Research, Gifu University, 1-1 Yanagido, Gifu 5010-1194, Japan

Contributed by Jack L. Strominger, August 11, 2008 (sent for review July 8, 2008)

Since the first determination of structure of the HLA-A2 complex, >200 MHC/peptide structures have been recorded, whereas the available T cell receptor (TCR)/peptide/MHC complex structures now are <20. Among these structures, only six are TCR/peptide/MHC Class II (MHCII) structures. The most recent of these structures, obtained by using TCR-Ob.1A12 from a multiple sclerosis patient and the MBP85–99/HLA-DR2 complex, was very unusual in that the TCR was located near the N-terminal end of the peptide-binding cleft of the MHCII protein and had an orthogonal angle on the peptide/MHC complex. The unusual structure suggested the possibility of a disturbance of its signaling capability that could be related to autoimmunity. Here, homology modeling and a new simulation method developed for TCR/peptide/MHC docking have been used to examine the positioning of the complex of two additional TCRs obtained from the same patient (TCR-Ob.2F3 or TCR-Ob.3D1 with MBP85–99/HLA-DR2). The structures obtained by this simulation are compatible with available data on peptide specificity of the TCR epitope. All three TCRs from patient Ob including that from the previously determined crystal structure show a counterclockwise rotation. Two of them are located near the N terminus of the peptide-binding cleft, whereas the third is near the center. These data are compatible with the hypothesis that the rotation of the TCRs may alter the downstream signaling.

human leukocyte antigen | multiple sclerosis | myelin basic protein | structural docking | signaling

The elucidation of structures of protein complexes is an arduous procedure particularly when the complexes are very large. The production of protein by recombinant techniques and subsequent crystallization of the complexes followed by x-ray diffraction analysis is a standard method. Structures can also be determined by NMR but that technique is presently limited to only relatively small proteins or complexes not >40–50 kDa. The third method, simulation of structures by homology modeling, has improved greatly in recent years. However, this technique is usable only when an appropriate template structure is available.

Crystallization and structure determination by x-ray diffraction of a MHC-encoded Class I (MHCI) protein/peptide complex was first accomplished in 1987 and MHCII in 1993 (1, 2). Since then, >200 structures of such complexes have been recorded (3). The β chain of the TCRs that recognize these complexes were first cloned in 1984 (4, 5), and the first structure of a TCR chain was published in 1995 (6). Approximately 40 complete TCR structures including both α and β chains are available now (3, 7). Similarly, the first TCR/peptide/MHC complex structures were published in 1996 (8, 9) but the number of such complex structures available now is <20 (3). Among these, only six are TCR/peptide/MHCII structures. The most recent of these structures is very unusual in that the TCR was located near the N-terminal end of the peptide-binding cleft of the MHCII protein and its orthogonal angle on the MHCII/peptide was 84° as compared with a diagonal angle of 40–53° for the other five structures (10). Also, it was rotated counterclockwise on the MHC molecule relative to the other structures. This

unusual structure suggested the possibility of a disturbance of its signaling capability that could be related to autoimmunity because this TCR, termed Ob.1A12 had been obtained from an autoreactive clone derived from a patient with multiple sclerosis (10). In fact, eight clones were obtained from this patient, two of which represent unique isolates (TCR-Ob.1A12 and TCR-Ob.3D1) and six of which have identical sequences, TCR-Ob.2F3 being an example (11).

In this article, we have used homology modeling of TCR structures on the appropriate templates and a new simulation method developed for TCR/peptide/MHC docking to examine the structures of the TCR/peptide/MHCII complexes of TCR-Ob.2F3 and TCR-Ob.3D1 in complex with the same MHC/peptide, namely HLA-DR2 (DRB1*1501/DRA) binding the myelin basic protein peptide epitope MBP85–99. MBP85–99 has previously been identified as the autoreactive peptide epitope in humans (12).

Results and Discussion

The AutoDock procedure was originally developed for docking studies of small chemicals to their receptors, for example the docking of a substrate to an enzyme (13). It makes use of charge and hydrophobicity calculations for both the receptor and the ligand (see *Materials and Methods*). By using this method in the present context, the peptide in question was first docked to the appropriate MHC molecule and separately to the TCR protein. The conformation of the peptide used in the docking in each case was taken from the crystal structure of the MBP85–99/HLA-DR2 (DRB1*1501, DRA) complex (10). After TCR/peptide and peptide/MHC structures were simulated, the two structures were merged by using the conformation of the peptide as the basis for merging. To validate the procedure, the technique was carried out by using two known TCR/peptide/MHC structures, that of the HLA-DR1 (DRB1*0101/DRA)/hemagglutinin (HA) 306–318 molecule in complex with the HLA-DR1-restricted HA306–318-specific TCR-HA1.7 (PDB ID code 1FYT) and then of the HLA-DR2/MBP85–99 molecule in complex with TCR-Ob.1A12 (PDB ID code 1YMM).

Simulated Structure of the TCR-HA1.7/HA306–318/HLA-DR1 Complex and the TCR-Ob.1A12/MBP85–99/HLA-DR2 Complex. The docking of HA306–318 to HLA-DR1 was simulated 10 times. Six of the 10 simulations showed exactly the same conformation inside the peptide-binding groove with energy equal to –33.8 kcal/mol (Fig. 1A). Four of the 10 showed different conformations binding outside of the groove with higher energies of –5.59, –5.59,

Author contributions: Z.K., J.N.H.S., K.K., N.K., and J.L.S. designed research; Z.K. and H.K.N. performed research; Z.K. and H.K.N. analyzed data; and Z.K., J.N.H.S., and J.L.S. wrote the paper.

The authors declare no conflict of interest.

To whom correspondence may be addressed. E-mail: zenkato@mac.com or jlstrom@fas.harvard.edu.

© 2008 by The National Academy of Sciences of the USA

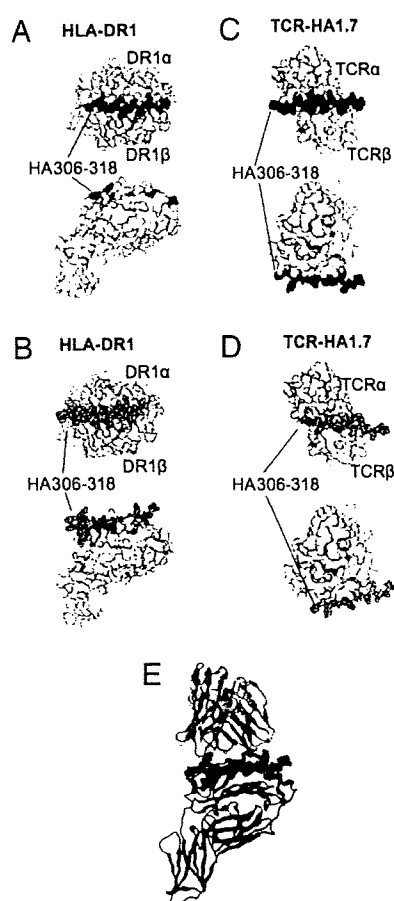


Fig. 1. Docking simulation of the HA306–318 peptide on HLA-DR1 and on TCR-HA1.7. (A) The six clustered docked peptides of HA306–318 on HLA-DR1 are indicated as space filling models in brown. (B) The four nonclustered docked peptides are indicated as space filling models in yellow. In A and B, HLA-DR1 (DRB1*0101/DRA) (20) is shown as a surface model in white. (C) The nine clustered docked peptides of HA306–318 on TCR-HA1.7 are indicated as space filling models in brown. (D) The one nonclustered docked peptide is shown as a space-filling model in yellow. In C and D, TCR-HA1.7 is shown as a surface model in white. (E) Merging of the docked TCR-HA1.7/HA306–318 and HA306–318/HLA-DR1 was carried out by using the conformation of the peptide as the basis for merging. Superposition was performed between the docked structure and the crystal structure of TCR-HA1.7/HA306–318/HLA-DR1 (20). Docked structure of TCR-HA1.7 in cyan, HA306–318 in brown, and crystal structures of both TCR-HA1.7 and HLA-DR1 in blue. The two TCR structures were superimposed by means of structures of HA306–318.

–5.68 and –8.73 kcal/mol (Fig. 1B). One of the clustered conformations inside the groove with the lowest energy was selected as representative.

Similarly, HA306–318 docking to TCR-HA1.7 was simulated 10 times. Nine of the 10 simulations had almost the same conformation with energy equal to –5.59 kcal/mol five times and energy –5.67 four times (Fig. 1C). One of the 10 simulations yielded a different conformation with a higher energy of –5.02 kcal/mol (Fig. 1D). Again, one of the five clustered conformations with the lowest energy was selected as representative.

Next, the TCR-HA1.7/HA306–318 simulated complex was merged with the HA306–318/HLA-DR1 simulated complex to give the TCR-HA1.7/HA306–318/HLA-DR1 complex by using the structure of the peptide as the basis for merging (a related procedure was used in a docking study of the dimeric maltose-binding complex involving maltose-binding protein and aspar-

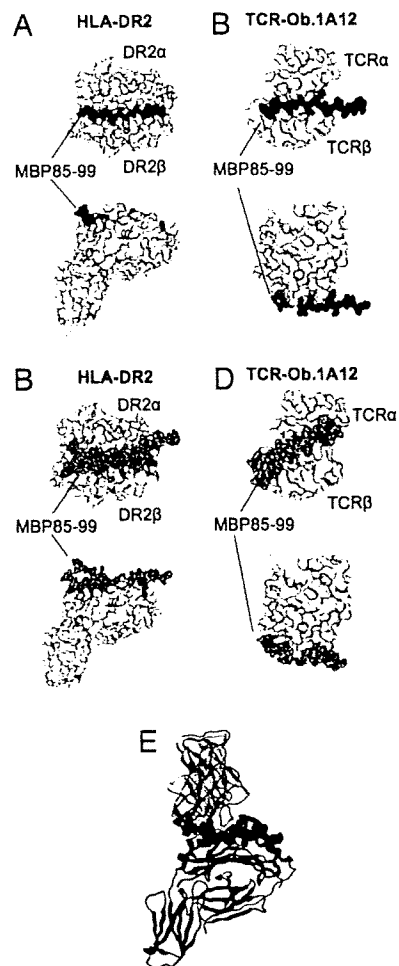


Fig. 2. Docking simulation of the MBP85–99 peptide on HLA-DR2 and on TCR-Ob.1A12. (A) The four clustered docked peptides of MBP85–99 on HLA-DR2 are indicated as space filling models in brown. (B) The six nonclustered docked peptides are indicated as space filling models in yellow. In A and B, HLA-DR2 (DRB1*1501/DRA) (10) is shown as a surface model in white. (C) The six clustered docked peptides of MBP85–99 on TCR-Ob.1A12 are indicated as space filling models in brown. (D) The four nonclustered docked peptides are indicated as space filling models in yellow. In C and D, TCR-Ob.1A12 is shown as a surface model in white. (E) Merging of the docked TCR-Ob.1A12/MBP85–99 and MBP85–99/HLA-DR2 was carried out by using the conformation of the peptide as the basis for merging. Superposition was performed between the docked structure and the crystal structure of TCR-Ob.1A12/MBP85–99/HLA-DR2 (10). Docked structure of TCR-Ob.1A12 in cyan, MBP85–99 in brown, and crystal structures of both TCR-Ob.1A12 and HLA-DR2 in blue. The two TCR structures were superimposed by means of structures of MBP85–99.

tate receptor, although in this case the octapeptide used was from a functional region of the maltose-binding protein) (14).

This simulated structure of the ternary complex was merged with the structure determined by crystallization and x-ray diffraction and gave excellent reproducibility with a rmsd of 1.64 Å (Fig. 1E). The same procedure was carried out to obtain the TCR-Ob.1A12/MBP85–99/HLA-DR2 structure. The docking of MBP85–99 to HLA-DR2 was simulated 10 times. Four of the 10 simulations showed exactly the same conformations inside the peptide-binding groove with energy equal to –26.8 kcal/mol (Fig. 2A). Six of the 10 showed binding outside of the groove each with a different conformation and with much higher energies of –3.02, –4.95, –4.95, –5.54, –5.64 and –5.91 kcal/mol (Fig. 2B). One of the clustered conformations inside the groove with the lowest energy was selected as representative.

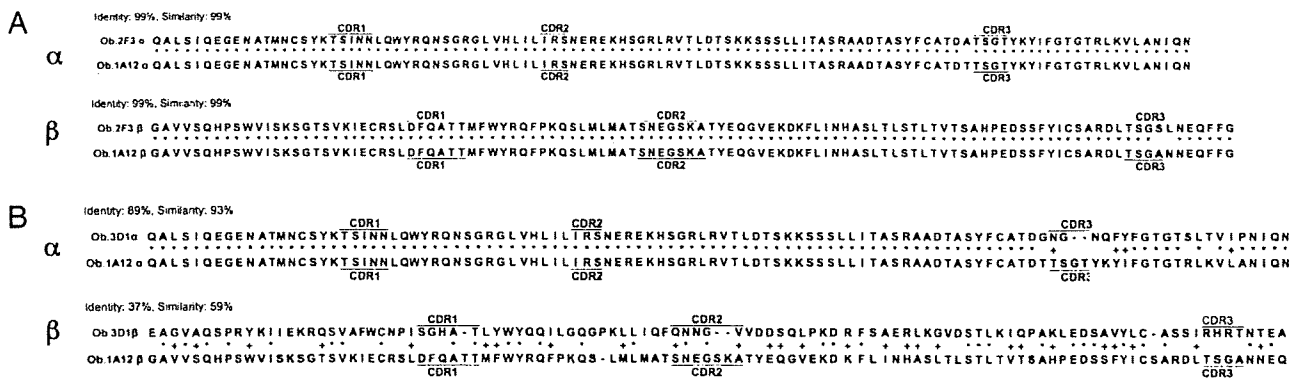


Fig. 3. Sequence alignment of TCR-Ob.2F3 and TCR-Ob.3D1 with TCR-Ob.1A12. (A) Sequence alignment between TCR-Ob.2F3 and TCR-Ob.1A12. (B) Sequence alignment between TCR-Ob.3D1 and TCR-Ob.1A12. Differences in amino acids between the two clones are indicated in yellow. *, identical amino acids; +, similar amino acids.

Similarly, MBP85–99 docking to TCR-Ob.1A12 was simulated 10 times. Six of the 10 simulations had almost the same conformation with energy equal to -4.78 five times and energy -4.65 once (Fig. 2C). Four of the 10 simulations each yielded a different conformation with a similar energy of -4.50 , -5.08 , -5.32 , and -5.32 kcal/mol (Fig. 2D). Again, one of the six clustered conformations with the lowest energy was selected as representative.

The TCR-Ob.1A12/MBP85–99 simulated complex was also merged with the MBP85–99/HLA-DR2 simulated complex as

described above to give the TCR-Ob1A12/MBP85–99/HLA-DR2 complex. Merging of the simulated structure with the structure determined by x-ray crystallography gave excellent reproducibility with a rmsd of 1.54 \AA (Fig. 2E). Thus, by using two known TCR/peptide/MHC complexes, these data provided a validation for the docking procedure used.

Notably, the energies of docking of the two peptides to their respective MHC proteins (-34 and -27 kcal/mol) were much lower than the energies of their docking to their respective TCR (-5.6

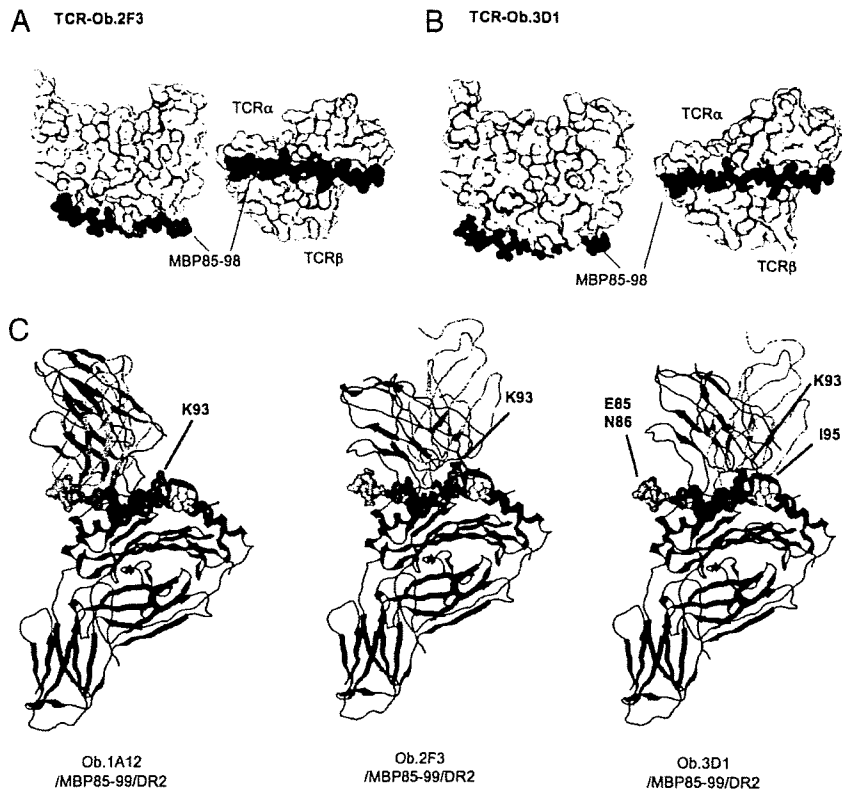


Fig. 4. Positioning of TCR-Ob.2F3 and TCR-Ob.3D1 on MBP85–99/HLA-DR2. (A) Docking simulation of the MBP85–99 peptide on TCR-Ob.2F3. The 10 clustered docked peptides are indicated as space filling models in brown. TCR-Ob.2F3 is shown as a surface model in white. (B) Docking simulation of the MBP85–99 peptide on TCR-Ob.3D1. The 10 clustered docked peptides are indicated as space filling models in brown. TCR-Ob.3D1 is shown as a surface model in white. (C) Comparison of positioning of the TCRs obtained from patient Ob. on the MBP85–99/HLA-DR2 structure. The structures of TCRs, MBP85–99 and HLA-DR2 (DRB1*1501/DRA) are shown as ribbon models. MBP85–99 and HLA-DR2 in blue, the α chains of the three TCRs in yellow, and the β chains of the three TCRs in red. Functionally important residues of MBP85–99 are shown as space filling models, E85 and N86 in green, V88 and K93 in orange, H90 and F91 in red, and I95 in yellow (see Results and Discussion).

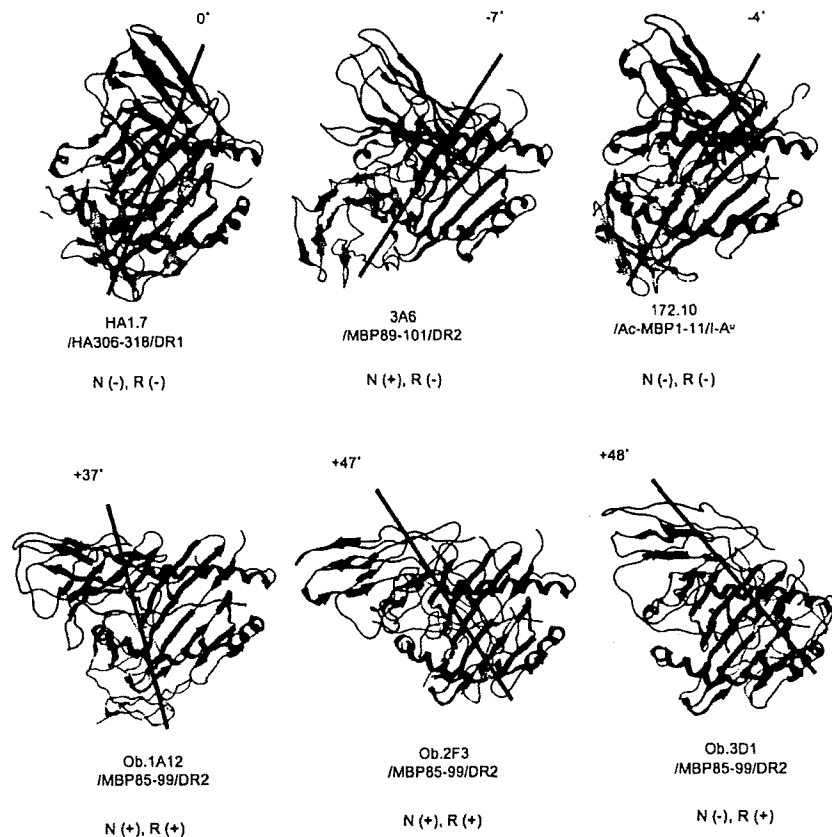


Fig. 5. Comparison of positioning between autoimmune TCRs and nonautoimmune TCR. HA1.7/HA306-318/DR1 indicates the positioning of a nonautoimmune TCR. All of the others are autoimmune TCRs. Black lines are drawn between the S-S bonds of TCR α and TCR β . Coloring is the same as in Fig. 4C. N, N-terminal shift; R, counterclockwise rotation. The degrees of rotation taking TCR-HA1.7 on HA306-318/HLA-DR1 as 0° were as follows: TCR-3A6, -7°; TCR-172.10, -4°; TCR-Ob.1A12, +37°; Ob.2F3, +47°; and TCR-Ob.3D1, +48°.

and -4.8 kcal/mol). Thus, the binding of the peptide to the MHC proteins is much stronger than the binding to the TCR (13).

Simulated Structure of the TCR-Ob.2F3/MBP85-99/HLA-DR2 Complex and the TCR-Ob.3D1/MBP85-99/HLA-DR2 Complex. Next, structures of two TCR complexes from patient Ob whose complexes with HLA-DR2/MBP85-99 had not been determined were modeled. The sequence alignment with the template TCR-Ob.1A12 of these two TCRs, TCR-Ob.2F3 and TCR-Ob.3D1, are shown in Fig. 3. Notably, TCR-Ob.2F3 has 99% sequence identity with TCR-Ob.1A12 differing at only three amino acid positions. One of these is near the CDR3 loop of the TCR α chain and the other two are in the CDR3 loop of the TCR β chain. By contrast, TCR-Ob.3D1 had only 89% identity in the TCR α chain differing from TCR-Ob.1A12 by 10 positions including two gaps. It had only 37% identity (but 59% similarity) in the β chain differing from the template structure by 40 aa including two insertions in the CDR3 loop.

When MBP85-99 was docked to the modeled TCR-Ob.2F3, the 10 simulations showed almost the same conformation with energies of -5.77 kcal/mol five times, -5.76 four times, and -5.75 once (Fig. 4A). One of the clustered conformations with the lowest energy was again selected as representative. The TCR-Ob.2F3/MBP85-99 docked structure was merged with the crystal structure of MBP85-99/HLA-DR2 again by using the conformation of the MBP85-99 peptide as the basis for merging.

Similarly, MBP85-99 was docked to the model TCR-Ob.3D1 10 times. All 10 simulations showed exactly the same conformation with energy -8.2 kcal/mol (Fig. 4B). One of these

clustered conformations was again selected as representative and as before docked with the MBP85-99/HLA-DR2 structure.

The structural models that resulted from these simulations are shown in Fig. 4C. Several features are obvious. First, like TCR-Ob.1A12 (10), TCR-Ob.2F3 is positioned toward the N-terminus of the peptide-binding groove. However, it is located very slightly more toward the C-terminal end of the peptide. With regard to rotation, the counterclockwise rotation of Ob.1A12 (+37°) as compared with HA1.7 (taken as 0°) is apparent (Fig. 5). The TCR-Ob.2F3 had an even greater counterclockwise rotation (+47°).

TCR-Ob.3D1 by contrast was located near the middle of the peptide-binding cleft at the apex of the helices in a similar position to TCR-HA1.7 (Figs. 4C and 5). However, again its counterclockwise rotation with regard to TCR-HA1.7 was large (+48°) and similar to that of TCR-Ob.2F3. When viewed from the top, the orthogonal angle of all three TCRs was distinct from that of HA1.7 and the other TCR/peptide/MHC complexes whose structures had been determined (5, 3, 15, 16). All three autoimmune TCRs show a counterclockwise rotation and two of them are located near the N-terminus of the peptide-binding cleft. These data are compatible with the hypothesis (10) that the rotation of the TCRs may alter the downstream signaling.

Available data on peptide specificity of the TCR epitope are compatible with these structures (Table 1, compiled from refs. 11, 12, 17, 18). With regard to the peptide, both TCR-Ob.1A12 and TCR-Ob.2F3 are sensitive to deletion of the N-terminal residue 85 of MBP85-99, whereas TCR-Ob.3D1 can recognize even a truncation of two residues at the N-terminus of

Table 1. Characters of the T cell clones from patient Ob

Clone	Ob.1A12	Ob.2F3	Ob.3D1
		Ob.1C3	
		Ob.1E10	
		Ob.1E12	
		Ob.1H8	
		Ob.2G9	
Minimal peptide	MBP 85–98	MBP 85–98	MBP 87–98
MBP 85–99	++++	++++	++++
MBP 85–98	++++	++++	++++
MBP 86–98	–	–	++++
MBP 87–98	–	–	++++
MBP 87–97	–	–	–
TCR epitope			
Major	HF—	HF-K–	HF-K–
Minor	—K–	—I	
MBP 85–99	++++	++++	++++
Val88Ala	++++	++++	ND
His90Ala	+	–	–
Phe91Ala	–	–	–
Lys93Ala	++++	++	–
Asn94Ala	++++	++	+
Ile95Ala	++++	+++	++
Val96Ala	++++	++++	++++

Plus symbol indicates the proliferation of the T cell clones. ND, Not determined. These data are derived from Wucherpfennig *et al.* (11), Wucherpfennig *et al.* (12), Hausmann *et al.* (17), and Wucherpfennig *et al.* (18).

MBP85–99 (Figs. 4C and 5). Alanine scanning of MBP85–99 revealed that TCR recognition of His-90 and Phe-91 was essential for all three clones (Table 1). Only TCR-Ob.3D1 was sensitive to mutation of Asn-94 (P6) or partially Ile-95 (P7), however, K93 was not essential for TCR-Ob.1A12, and K93A revealed reduced sensitivity at this residue for TCR-Ob.2F3 (Table 1). However, both K93A and N94A eliminated reactivity with TCR-Ob.3D1 and I95A reduced reactivity. These data are compatible with the positions of the three TCR as shown in Figs. 4C and 5. Thus, good structure-function correlations are observed in the three autoimmune T cell clones.

The CD4 coreceptor binds to the membrane-proximal MHCII domains and is essential for T cell development and T cell function by recruiting the tyrosine kinase Lck. The alignment of the TCRs observed here showed that the geometry of the interaction with the CD4 coreceptor is altered for the TCRs as previously suggested (10). These findings raise the possibility that CD4 function is affected in immature T cells by an altered geometry of TCR binding to peptide-MHC during the formation of immunological synapses (10). These structures may add to our understanding of the molecular mechanism that could relate to autoimmunity.

Materials and Methods

Structure Modeling of TCR. Structural modeling of TCR-Ob.2F3 and TCR-Ob.3D1 was performed by using MOE software (Chemical Computing Group, www.chemcomp.com) combined with the segment-matching procedure (19, 20). Briefly, the structure of TCR-Ob.1A12 complexed with MBP85–99/HLA-DR2 (10) (PDB ID code 1YMM) was used as a template for homology modeling

- Bjorkman PJ, *et al.* (1987) The foreign antigen binding site and T cell recognition regions of class II histocompatibility antigens. *Nature* 329:512–518.
- Brown JH, Jardetzky TS, Gorga JC, Stern LJ, Urban RG (1993) Three-dimensional structure of the human class II histocompatibility antigen HLA-DR1. *Nature* 364:33–39.
- Rudolph MG, Stanfield RL, Wilson IA (2006) How TCRs bind MHCs, peptides, and coreceptors. *Annu Rev Immunol* 24:419–466.
- Hedrick SM, Cohen DI, Nielsen EA, Davis MM (1984) Isolation of cDNA clones encoding T cell-specific membrane-associated proteins. *Nature* 308:149–153.
- Yanagi Y, *et al.* (1984) A human T cell-specific cDNA clone encodes a protein having extensive homology to immunoglobulin chains. *Nature* 308:145–149.

of TCR-Ob.2F3 and TCR-Ob.3D1. The modeled structure was further energy minimized (MOE software).

Docking Studies of the TCR with Peptide/MHC. Docking was performed by using the AutoDock software package running on Intel-based Xeon, ppcDarwin platform (13). The structure of HLA-DR1 (DRB1*0101/DRA), HLA-DR2 (DRB1*1501/DRA), TCR-HA1.7, TCR-Ob.1A12, TCR-Ob.2F3, or TCR-Ob.3D1 was used as the target structure. HA306–318 or MBP85–99 in the conformation found in their crystal structures (10, 21) was used as the ligand structure. AutoDock with a Lamarckian genetic search algorithm (LGA) was chosen for all dockings (13).

The optimized AutoDocking run parameters were similar to those described in ref. 13 with minor modification in grid size, a maximum number of energy evaluations, and a maximum number of generations. The proteins and ligands in the dockings were treated by using the united-atom approximation. Only polar hydrogens were added to the protein, and Kollman united-atom partial charges were assigned. All waters were removed. Atomic solvation parameters and fragmental volumes were assigned to the protein atoms by using an AUTODOCK utility, ADDSOL and the grid maps were calculated by using AUTOGRID (13).

The dimensions of the grids for docking were thus 180 × 80 × 90 points (67.5 Å × 30.0 Å × 33.7 Å) and a grid-point spacing of 0.375 Å, and the center of the grids were placed to cover the surface of the HLA or TCR structure. The ligand was treated initially as all atom entities, i.e., all hydrogens were added, then partial atomic charges were calculated by using the Gasteiger-Marsili method (13). AUTOTORS, an AUTODOCK utility, was used to define the rotatable bonds in the ligand to unite the nonpolar hydrogens added by SYBYL for the partial atomic charge calculation. The partial charges on the nonpolar hydrogens were added to that of the hydrogen-bearing carbon also in AUTOTORS.

In the analyses, 10 dockings were performed; in the analysis of the docked conformations, the clustering tolerance as different conformations for the rmsd was 1.0 Å. The step sizes were 0.2 Å for translations and 5° for orientations and torsions. The α and β parameters determined the size of the mutation in the genetic algorithms, LGA. The Cauchy distribution parameters were: $\alpha = 0$ and $\beta = 1$. Note that random changes were generated in the genetic algorithm by a Cauchy distribution.

In the LGA dockings, an initial population of random individuals with a population size of 50 individuals was used; a maximum number of 2.5×10^8 energy evaluations; a maximum number of generations of 2.7×10^4 ; an elitism value of 1, which was the number of top individuals that automatically survived into the next generation; a mutation rate of 0.02, which was the probability that a gene would undergo a random change; and a cross-over rate of 0.80, which was the probability that two individuals would undergo cross-over. Proportional selection was used, where the average of the worst energy was calculated over a window of the previous 10 generations. In the LGA dockings, the pseudoSolis and Wets local search method was used, having a maximum of 300 iterations per local search; the probability of performing local search on an individual in the population was 0.06; the maximum number of consecutive successes or failures before doubling or halving the local search step size, r , was 4, in both cases; and the lower bound on r , the termination criterion for the local search, was 0.01.

TCR/Peptide/MHC Complex Structure. To make the whole TCR/peptide/MHC complex structure, superposition was done between the docked structure of the TCR/peptide and the docked structure of peptide/HLA or between the docked structure of the TCR/peptide and the crystal structure of the peptide/HLA complex. Then, the peptide structure was removed from the system. The structures obtained were further energy-minimized (MOE software).

ACKNOWLEDGMENTS. We thank M. Karplus for technical advice and D. Keskin for helpful comments. This work was supported by National Institutes of Health Research Grant 5R01 AI049524 and National Multiple Sclerosis Society Award RG3796A3.

- Bentley GA, Boulot G, Karjalainen K, Mariuzza RA (1995) Crystal structure of the beta chain of a T cell antigen receptor. *Science* 267:1984–1987.
- Mak TW (2007) The T cell antigen receptor: "The Hunting of the Snark." *Eur J Immunol* 37(Suppl 1):S83–S93.
- Garboczi DN, *et al.* (1996) Structure of the complex between human T-cell receptor, viral peptide and HLA-A2. *Nature* 384:134–141.
- Garcia KC, *et al.* (1996) An alpha-beta T cell receptor structure at 2.5 Å and its orientation in the TCR-MHC complex. *Science* 274:209–219.
- Hahn M, Nicholson MJ, Pyrdol J, Wucherpfennig KW (2005) Unconventional topology of self peptide-major histocompatibility complex binding by a human autoimmune T cell receptor. *Nat Immunol* 6:490–496.

11. Wucherpfennig KW, et al. (1994) Clonal expansion and persistence of human T cells specific for an immunodominant myelin basic protein peptide. *J Immunol* 152:5581–5592.
12. Wucherpfennig KW, et al. (1994) Structural requirements for binding of an immunodominant myelin basic protein peptide to DR2 isotypes and for its recognition by human T cell clones. *J Exp Med* 179:279–290.
13. Morris GM, Goodsell DS, Huey R, Olson AJ (1996) Distributed automated docking of flexible ligands to proteins: Parallel applications of AutoDock 2.4. *J Comput Aided Mol Des* 10:293–304.
14. Stoddard BL, Koshland DE, Jr (1992) Prediction of the structure of a receptor-protein complex using a binary docking method. *Nature* 358:774–776.
15. Maynard J, et al. (2005) Structure of an autoimmune T cell receptor complexed with class II peptide-MHC: Insights into MHC bias and antigen specificity. *Immunity* 22:81–92.
16. Li Y, et al. (2005) Structure of a human autoimmune TCR bound to a myelin basic protein self-peptide and a multiple sclerosis-associated MHC class II molecule. *EMBO J* 24:2968–2979.
17. Hausmann S, Martin M, Gauthier L, Wucherpfennig KW (1999) Structural features of autoreactive TCR that determine the degree of degeneracy in peptide recognition. *J Immunol* 162:338–344.
18. Wucherpfennig KW, Hafler DA, Strominger JL (1995) Structure of human T-cell receptors specific for an immunodominant myelin basic protein peptide: Positioning of T-cell receptors on HLA-DR2/peptide complexes. *Proc Natl Acad Sci USA* 92:8896–8900.
19. Fechteler T, Dengler U, Schomberg D (1995) Prediction of Protein Three-Dimensional Structures in Insertion and Deletion Regions: A Procedure for Searching Databases of Representative Protein Fragments Using Geometric Scoring Criteria. *J Mol Biol* 253:114–131.
20. Levitt M (1992) Accurate Modeling of Protein Conformation by Automatic Segment Matching. *J Mol Biol* 226:507–533.
21. Henneke J, Carfi A, Wiley DC (2000) Structure of a covalently stabilized complex of a human $\alpha\beta$ T-cell receptor, influenza HA peptide and MHCII molecule, HLA-DR1. *EMBO J* 19:5611–5624.

IL-10 plays an important role as an immune-modulator in the pathogenesis of atopic diseases

MINAKO KAWAMOTO, EIKO MATSUI, HIDEO KANEKO, TOSHIYUKI FUKAO,
TAKAHIDE TERAMOTO, KIMIKO KASAHARA and NAOMI KONDO

Department of Pediatrics, Graduate School of Medicine, Gifu University, Gifu, Japan

Received July 7, 2008; Accepted September 15, 2008

DOI: 10.3892/mmr_00000037

Abstract. Interleukin (IL)-10 has anti-inflammatory activities in various immune reactions and plays an important role in the regulation of immune diseases. In the present study, we examined the role of IL-10 in atopic diseases. Peripheral blood mononuclear cells (PBMCs) from healthy control subjects, patients with atopic dermatitis and patients with bronchial asthma were cultured with lipopolysaccharide (LPS). The production of IL-10, IL-12 or IFN- γ by PBMCs stimulated with LPS was measured. Next, we investigated whether the haplotype in the *IL-10* gene promoter region had an effect on the production of IL-10 by PBMCs. PBMCs from patients were cultured with phytohemagglutinin, to which recombinant human IL-10 had been added. IL-12, IFN- γ and IL-4 production by PBMCs was measured. β -lactoglobulin (BLG)-specific T cell clones were cultured with BLG peptide (P-17), antigen-presenting cells and recombinant human IL-10. The antigen-induced proliferation of the T cell clones and cytokine production were assayed. Results demonstrated that IL-10 production by LPS-stimulated PBMCs was lower in atopic patients than in healthy control subjects. Three different haplotypes in the *IL-10* gene promoter region were detected. These haplotypes did not correlate with IL-10 production by PBMCs. IL-10 inhibited Th1 cytokine production by PBMCs, and also inhibited the antigen-induced proliferation of T cell clones and Th2 cytokine production. In conclusion, IL-10 inhibits both the production of Th1 and Th2 cytokines and the antigen-induced proliferation of T cell clones. Thus, IL-10

modulates other cytokines and plays an important role as an immune-modulator in the pathogenesis of atopic diseases.

Introduction

Interleukin (IL)-10, which is a homodimeric cytokine produced by activated monocytes, macrophages, mast cells and T cells, is deeply involved in the regulation of inflammatory responses and immune reactions. IL-10 was originally described as an inhibitory factor produced by murine Th2 cells that suppresses interferon- γ (IFN- γ) production by activated murine Th1 cells (1-3). Later, studies demonstrated IL-10 to be a potent inhibitor of monocyte and macrophage functions, suppressing the production of many pro-inflammatory cytokines and chemokines (4-7).

Several studies demonstrated that IL-10 has an important role in the pathogenesis of inflammatory bowel disease and autoimmune diseases, such as rheumatoid arthritis, systemic lupus erythematosus and multiple sclerosis (8,9). These diseases are called Th1-mediated diseases, as Th1 cytokines play a central role in their inflammation.

Recently, studies have revealed that IL-10 is associated with the pathogenesis of Th2-mediated diseases, such as allergic diseases. Therefore, we investigated the involvement of IL-10 in allergic reactions.

Materials and methods

Atopic patients and control subjects. Twelve healthy control subjects and 31 patients with atopic disease were studied. The serum IgE levels and radioallergosorbent test (RAST) scores of 12 healthy control subjects, 12 patients with atopic dermatitis (AD) and 19 patients with bronchial asthma (BA) are listed in Table I. AD was diagnosed according to the criteria of Haniffin, and BA according to the criteria of The American Thoracic Society. The healthy control subjects had a negative history of atopic disease, and their serum IgE levels were within normal limits for their age. They were moreover healthy and free of any acute infections at blood sampling. The subjects were randomly selected through our hospital, and informed consent was obtained from all subjects or their parents.

Cell preparation. PBMCs were isolated from the heparinized blood samples of healthy control subjects and atopic patients by gradient centrifugation using Ficoll-Paque (Pharmacia,

Correspondence to: Dr Minako Kawamoto, Department of Pediatrics, Graduate School of Medicine, Gifu University, 1-1 Yanagido, Gifu 501-1194, Japan
E-mail: mina@gifu-u.ac.jp

Abbreviations: AD, atopic dermatitis; BA, bronchial asthma; IL-10, interleukin-10; IL-12, interleukin-12; IFN- γ , interferon- γ ; Th1, helper T cell type 1; Th2, helper T cell type 2; BLG, β -lactoglobulin; PBMCs, peripheral blood mononuclear cells

Key words: interleukin-10, atopic dermatitis, bronchial asthma, peripheral blood mononuclear cells, T cell clone, *interleukin-10* gene

Uppsala, Sweden). PBMCs were suspended at a density of 10^6 /ml in RPMI-1640 medium supplemented with 10% heat-inactive fetal calf serum, 2 mmol/l L-glutamine, 100 U/ml penicillin and 100 mg/ μ l streptomycin (10).

Cell culture. PBMCs (10^6 /ml) were cultured with 1 μ g/ml lipopolysaccharide (LPS) (Sigma, St. Louis, MO, USA) for 24 h in a volume of 1 ml in a round-bottom tube (Falcon 2059, Becton Dickinson Labware, Lincoln Park, NJ, USA) at 37°C in a humidified atmosphere containing 5% CO₂.

PBMCs (10^6 /ml) from one randomly selected healthy control subject, one AD patient and three BA patients were cultured with 10 μ g/ml phytohemagglutinin (PHA) (Gibco BRL, Grand Island, NY, USA) or 1 μ g/ml LPS and recombinant human IL-10 (Genzyme, Minneapolis, MN, USA) at 0.1, 0.5, 1, 5, 10, 20 or 100 ng/ml for 24 h in a volume of 1 ml in a round-bottom tube.

Antigen-induced proliferative responses and cytokine production of BLG-specific T cell clones. β -lactoglobulin (BLG)-specific T cell clones were used as described previously (11). The antigen-induced proliferation of the T cell clones was assayed by culturing T cells (2×10^4 /well) in 96-well flat-bottomed culture plates with the BLG peptide (P-17) and 3000 cGy-irradiated autologous PBMCs (1.5×10^5 /well) as antigen-presenting cells (APCs) and recombinant human IL-10, (0.1, 1, 10 or 100 ng/ml) or recombinant human TGF- β , (0.001, 0.01, 0.1, 1 or 10 ng/ml). Cells were cultured for 72 h with 1 μ Ci/well of [³H] TdR during the final 16-h period, and the incorporated radioactivity was measured by liquid scintillation counting. To assay cytokine production, culture supernatants in 96-well flat-bottomed tubes were spun to remove cells after the cultures and were stored at -80°C until used for assay.

Cytokine assays. IL-10 concentration was measured with a human IL-10 enzyme-linked immunosorbent assay (ELISA) kit (BioSource International, CA, USA) with a detection limit of 15.6 pg/ml. IL-12 concentration was measured with a human IL-12 ELISA kit (BioSource International) with a detection limit of 7.81 pg/ml. IFN- γ concentration was measured with a human IFN- γ ELISA kit (Ohtsuka, Tokyo, Japan) with a detection limit of 15.6 pg/ml, and IL-4 concentration was measured with a human IL-4 ultrasensitive ELISA kit (BioSource International) with a detection limit of 0.39 pg/ml. Lastly, IL-5 concentration was measured with a human IL-5 ELISA kit (Bio Source International) with a detection limit of 11.7 pg/ml.

Detection of polymorphisms in the IL-10 gene. Genomic DNA was extracted from neutrophils with a Sepagene kit (Sanko Junyaku, Tokyo, Japan). The promoter region and five exons of the IL-10 gene (Gene Bank accession no. U16720) were amplified and sequenced using an ABI PRISM 377 DNA sequencer.

Statistical analyses. The significance of the differences between groups was analyzed using the Mann-Whitney U test. Probability (p) values <0.05 were considered statistically significant.

Table I. Clinical features of the 43 subjects.

	Age (years)	Gender	Diagnosis	Serum IgE (IU/ml)	RAST scores	
					HD	Derf
Control subjects						
1	11	M	Healthy	5.7	0	0
2	1	M	Healthy	5.9	0	0
3	1	F	Healthy	11.0	0	0
4	1	M	Healthy	15.0	0	0
5	1	M	Healthy	25.0	0	0
6	1	F	Healthy	29.1	0	1
7	6	F	Healthy	58.0	0	0
8	5	F	Healthy	70.0	0	0
9	2	M	Healthy	72.0	0	0
10	4	F	Healthy	98.3	1	0
11	5	M	Healthy	100.0	0	0
12	1	F	Healthy	110.0	0	0
Atopic patients						
1	1	M	AD	16.8	2	3
2	0	M	AD	236.0	0	0
3	3	M	AD	1,123.1	5	6
4	3	F	AD	2,024.7	6	6
5	1	M	AD	2,586.5	3	1
6	13	M	AD	2,769.0	3	3
7	1	M	AD	3,476.0	5	4
8	4	F	AD	3,782.6	6	6
9	3	F	AD	4,514.1	6	6
10	6	F	AD	5,500.0	6	6
11	5	M	AD	6,729.9	6	6
12	1	F	AD	14,666.3	3	3
13	5	M	BA	114.6	4	5
14	2	F	BA	127.6	4	4
15	2	F	BA	148.0	4	4
16	3	F	BA	251.4	5	5
17	7	F	BA	267.7	3	4
18	4	M	BA	300.0	0	0
19	11	M	BA	451.0	5	5
20	14	F	BA	484.0	5	5
21	10	M	BA	516.5	5	5
22	9	M	BA	517.5	6	6
23	3	F	BA	545.2	6	6
24	6	M	BA	616.3	1	1
25	9	M	BA	669.9	3	3
26	14	M	BA	839.0	5	5
27	8	M	BA	907.0	6	6
28	12	F	BA	1,581.6	2	2
29	8	M	BA	1,700.0	6	5
30	13	M	BA	3,063.9	6	6
31	9	F	BA	3,860.6	3	4

AD, atopic dermatitis; BA, bronchial asthma. M, male; F, female. HD, house dust; Derf, *Dermatofagoides farinae*.

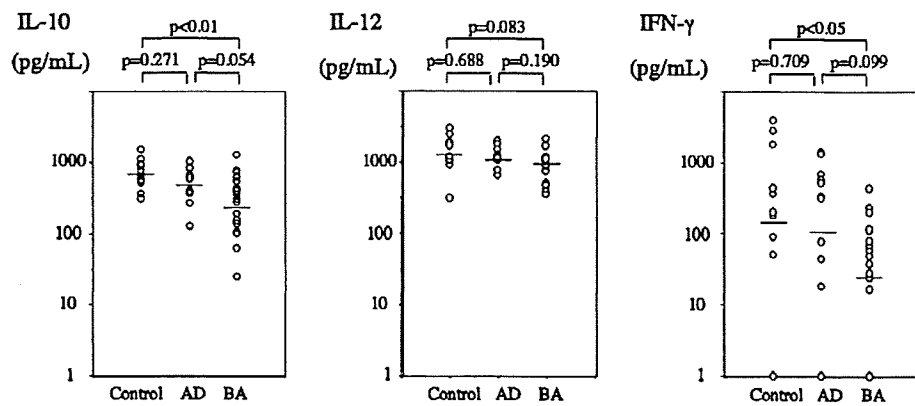


Figure 1. IL-10, IL-12 or IFN- γ production by LPS-stimulated PBMCs in healthy control subjects (n=12), AD (n=12) and BA patients (n=19).

Table II. The prevalence of haplotypes in the *IL-10* gene.

Haplotype	GCC	ACC	ATA
Control (n=10)	0 (0%)	4 (20.0%)	16 (80.0%)
AD (n=10)	0 (0%)	5 (25.0%)	15 (75.0%)
BA (n=13)	2 (7.7%)	7 (26.9%)	17 (65.4%)

AD, atopic dermatitis; BA, bronchial asthma.

Results

IL-10 production by PBMCs in atopic patients and healthy control subjects. We studied IL-10 production by PBMCs in atopic patients and healthy control subjects. Twelve healthy control subjects, 12 patients with AD and 19 patients with BA were studied. IL-10, IL-12 and IFN- γ production by LPS-stimulated PBMCs was measured with ELISA kits. The features of the patients are summarized in Table I.

IL-10 production by PBMCs stimulated with LPS is shown in Fig. 1. IL-10 production was lower in atopic patients than in healthy control subjects. In particular, IL-10 production was lower in patients with BA (average, 275.4 pg/ml; 1 SD range, 102.3-741.3 pg/ml) than in healthy control subjects (average, 691.8 pg/ml; 1 SD range, 446.7-1071.5 pg/ml) ($p < 0.01$) (Fig. 1). IFN- γ production was also lower in patients with BA than in healthy control subjects. IL-10, IL-12 and IFN- γ production was lower in patients with AD than that in control subjects, but there was no statistically significant difference between the two groups when analyzed using the Mann-Whitney U test.

IL-10 gene polymorphisms and atopic diseases. The *IL-10* gene from allergic patients and healthy control subjects was sequenced. We detected three polymorphisms in the *IL-10* gene promoter region, -1082 (G/A), -819 (C/T) and -592 (C/A) as previously reported (12,13). These polymorphisms produced three different haplotypes, GCC, ACC and ATA.

We determined the prevalence of these haplotypes in the *IL-10* gene in both allergic patients and healthy control subjects

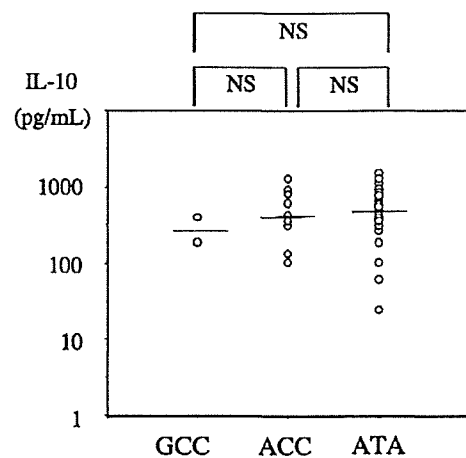


Figure 2. Relationship between the haplotype of the *IL-10* gene promoter region and IL-10 production by LPS-stimulated PBMCs.

by direct sequencing (Table II). None of the healthy control subjects or AD patients had the GCC haplotype. Two of the BA patients had the GCC haplotype. Most of the healthy control subjects and atopic patients had the ATA haplotype.

Next, we investigated whether these polymorphisms were associated with the production of IL-10 by LPS-stimulated PBMCs. As shown in Fig. 2, these polymorphisms did not have an effect on IL-10 production by PBMCs in this study.

Effect of IL-10 on Th1 and Th2 cytokine production by PBMCs. The effect of IL-10 on Th1 and Th2 cytokine production in atopic patients was examined. IFN- γ production by PBMCs stimulated with PHA was significantly inhibited by IL-10 in a dose-dependent manner (Fig. 3A). Similarly, IL-12 production by PBMCs stimulated with PHA was inhibited by IL-10 in a dose-dependent manner (Fig. 3B). IL-12 production by PBMCs stimulated with LPS was inhibited by IL-10 (data not shown). These data suggest that the production of Th1 cytokines such as IL-12 and IFN- γ by PBMCs are directly inhibited by IL-10.

Furthermore, we investigated the effect of IL-10 on the production of the Th2 cytokine IL-4. IL-4 production by

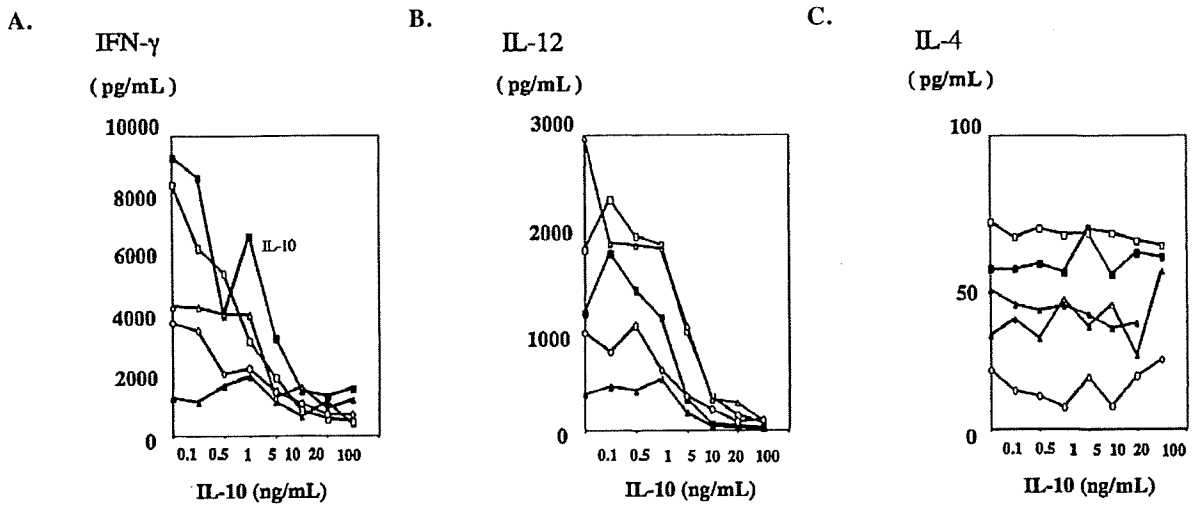


Figure 3. Effect of IL-10 on IL-12, IFN- γ or IL-4 production by PHA-stimulated PBMCs in one randomly selected healthy control subject, one AD patient and three BA patients (control subject -■-, AD patient -▲-, BA patient 1 -□-, BA patient 2 -△-, BA patient 3 -◇-). (A) IFN- γ production by PHA-stimulated PBMCs was inhibited by IL-10 dose-dependently in one healthy control subject and three BA patients. In one AD patient, IFN- γ production by PHA-stimulated PBMCs was low and was not evaluated. (B) IL-12 production by PHA-stimulated PBMCs was inhibited by IL-10 dose-dependently in all patients. (C) IL-4 production by PHA-stimulated PBMCs was not affected by IL-10.

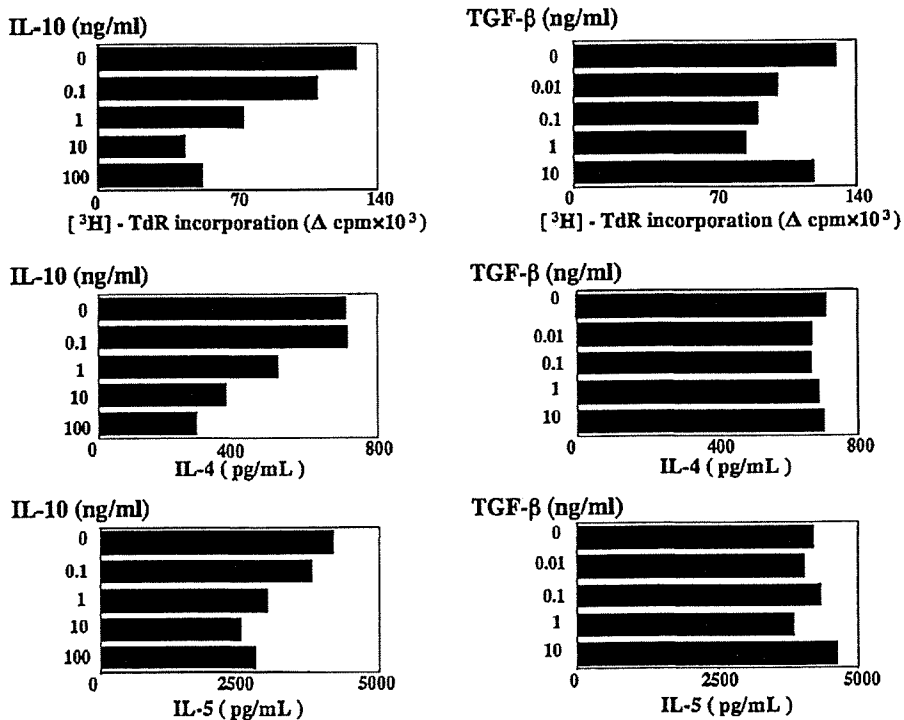


Figure 4. Antigen-induced proliferative responses and cytokine production of β -lactoglobulin (BLG)-specific T cell clones. IL-10 inhibited the BLG-specific antigen-induced proliferation of T cell clones. IL-10 also inhibited the production of IL-4 and IL-5 by T cell clones.

PBMCs stimulated with PHA did not change with the addition of IL-10 (Fig. 3C).

Effect of IL-10 on specific antigen-induced proliferation of T cell clones. The effect of IL-10 on specific antigen-induced proliferation of T cell clones and Th2 cytokine production by T cell clones was examined. The BLG-specific antigen-

induced proliferation of T cell clones was significantly inhibited by IL-10 in a dose-dependent manner (Fig. 4). In contrast, TGF- β did not inhibit the proliferation of T cell clones.

Furthermore, IL-10 inhibited the production of the Th2 cytokines IL-4 and IL-5 by T cell clones in a dose-dependent manner (Fig. 4).

Discussion

Immune responses generated by cytokines are essential to the development of allergic disease (14). IL-4, IL-5 and IL-13 produced by Th2 cells induce, prolong and amplify allergic responses by enhancing the production of IgE and the recruitment, growth and differentiation of eosinophils and mast cells. They also directly cause airway hyperreactivity in and of themselves. It has been suggested that Th2-mediated allergic diseases result from inadequate Th1 cytokine production. Our previous studies demonstrated that IL-12 and IFN- γ play important roles in the regulation of IgE synthesis by B cells (15,16).

IL-10 is an anti-inflammatory cytokine. Human IL-10, in contrast to murine IL-10 (which is primarily a Th2 product), is produced by both the Th1 and Th2 cells (17) as well as by mononuclear phagocytes, which may be its most important source (18). A role for IL-10 in the regulation of immune responses to allergens was first suggested by studies revealing that IL-10 inhibited cytokine production by eosinophils stimulated with LPS (19). Later, it was demonstrated that IL-10 might also inhibit the production of cytokines, such as TNF and IL-6, by stimulated mast cells (20,21). IL-10 inhibits monocyte major histocompatibility complex-class (MHC-class II), B7.1 (CD80), B7.2 (CD88), intercellular adhesion molecule-1, and CD23 expression and accessory cell function (22). Monocytes pre-treated with IL-10 fail to induce specific antigen T cell proliferation.

In this study, IL-10 production by PBMCs in atopic patients, particularly BA patients, was significantly lower than in healthy control subjects. This might be explained by reduced IL-10 production, which was noted in the lungs of asthmatic patients as a result of a decreased gene expression level (23,24).

Next, we investigated whether the difference in IL-10 production between healthy control subjects and atopic patients was due to a difference in the distribution of the haplotype in the *IL-10* gene promoter region. In a previous study, the GCC/GCC genotype was associated with higher production and the ATA haplotype with lower production of IL-10 by PBMCs compared with other genotypes. However, none of our subjects had the GCC/GCC genotype. Most of the healthy control subjects and atopic patients had the ATA haplotype. Two of the BA patients had the GCC haplotype. IL-10 production by PBMCs was not affected by these haplotypes of the *IL-10* gene promoter region. Lim *et al* reported that the IL-10 haplotype has a role in determining disease severity, but does not seem to be important to disease susceptibility (12). More studies are required to clarify these points.

Lastly, we investigated the effect of IL-10 on the Th1 or Th2 cytokines. In this study, IFN- γ and IL-12 production by PBMCs stimulated with PHA were inhibited by IL-10. IL-12 production by PBMCs stimulated with LPS was also inhibited by IL-10. These data suggest that IL-10 is an inhibitor of Th1 cytokines. Moreover, IL-10 inhibited the antigen-induced proliferation of T cell clones and Th2 cytokine production by T cell clones. Previous studies have demonstrated that IL-10 inhibits cytokine production and the proliferation of CD4⁺ T cells and T cell clones via down-regulatory effects on APC function (2,25). In addition, IL-10 directly affects the function of T cells and inhibits IL-4 and

IL-5 production depending on activation conditions (26). It is reported that IL-10 production by regulatory T cells (CD4⁺/CD25⁺ T cells) plays an important role in the regulation of allergies by inhibiting Th0, Th1 and Th2 cells (27,28). Recently, it was reported that IL-10 and IL-13R α 2 coordinately suppressed Th2-mediated inflammation and pathology, respectively (29).

IL-10 could play a critical role in the pathogenesis of atopic diseases and is a modulator of Th1 and Th2 cytokines. However, further research into the function of IL-10 is required.

References

1. Fiorentino DF, Bond MW and Mosmann TR: Two types of mouse T helper cell. IV. Th2 clones secrete a factor that inhibits cytokine production by Th1 clones. *J Exp Med* 170: 2081-2095, 1989.
2. Fiorentino DF, Zlotnik A, Vieira P, Mosmann TR, Howard M, Moore KW and O'Garra A: IL-10 acts on the antigen-presenting cell to inhibit cytokine production by Th1 cells. *J Immunol* 146: 3444-3451, 1991.
3. D'Andrea A, Aste-Amezaga M, Valiante NM, Ma X, Kubin M and Trinchieri G: Interleukin 10 (IL-10) inhibits human lymphocyte interferon- γ production by suppressing natural killer cell stimulatory factor/IL-12 synthesis in accessory cells. *J Exp Med* 178: 1041-1048, 1993.
4. Fiorentino DF, Zlotnik A, Mosmann TR, Howard M and O'Garra A: IL-10 inhibits cytokine production by activated macrophages. *J Immunol* 147: 3815-3822, 1991.
5. Gruber MF, Williams CC and Gerrard TL: Macrophage-colony-stimulating factor expression by anti-CD45 stimulated human monocytes is transcriptionally up-regulated by IL-1 beta and inhibited by IL-4 and IL-10. *J Immunol* 152: 1354-1361, 1994.
6. Marfaing-Koka A, Maravic M, Humbert M, Galanaud P and Emilie D: Contrasting effects of IL-4, IL-10 and corticosteroids on RANTES production by human monocytes. *Int Immunol* 8: 1587-1594, 1996.
7. Kopydlowski KM, Salkowski CA, Cody MJ, van Rooijen N, Major J, Hamilton TA and Vogel SN: Regulation of macrophage chemokine expression by lipopolysaccharide in vitro and in vivo. *J Immunol* 163: 1537-1544, 1999.
8. Gasche C, Bakos S, Dejaco C, Tillinger W, Zakeri S and Reinisch W: IL-10 secretion and sensitivity in normal human intestine and inflammatory bowel disease. *J Clin Immunol* 20: 362-370, 2000.
9. Grondal G, Gunnarsson I, Ronnelid J, Rogberg S, Klareskog L and Lundberg I: Cytokine production, serum levels and disease activity in systemic lupus erythematosus. *Clin Exp Rheumatol* 18: 565-570, 2000.
10. Kondo N, Fukutomi O, Agata H, Motoyoshi F, Shinoda S, Kobayashi Y, Kuwabara N, Kameyama T and Orii T: The role of T lymphocytes in patients with food-sensitive atopic dermatitis. *J Allergy Clin Immunol* 91: 658-668, 1993.
11. Sakaguchi H, Inoue R, Kaneko H, Watanabe M, Suzuki K, Kato Z, Matsushita S and Kondo N: Interaction among human leucocyte antigen-peptide-T cell receptor complexes in cow's milk allergy: the significance of human leucocyte antigen and T cell receptor-complementarity determining region 3 loops. *Clin Exp Allergy* 32: 762-770, 2002.
12. Lim S, Crawley E, Woo P and Barnes PJ: Haplotype associated with low interleukin-10 production in patients with severe asthma. *Lancet* 352: 113, 1998.
13. Turner DM, Williams DM, Sankaran D, Lazarus M, Sinnott PJ and Hutchinson IV: An investigation of polymorphism in the interleukin-10 gene promoter. *Eur J Immunogenet* 24: 1-8, 1997.
14. Umetsu DT and DeKruyff RH: TH1 and TH2 CD4⁺ cells in human allergic diseases. *J Allergy Clin Immunol* 100: 1-6, 1997.
15. Teramoto T, Fukao T, Tashita H, Inoue R, Kaneko H, Takemura M and Kondo N: Serum IgE level is negatively correlated with the ability of peripheral mononuclear cells to produce interferon gamma (IFN- γ): evidence of reduced expression of IFN- γ mRNA in atopic patients. *Clin Exp Allergy* 28: 74-82, 1998.
16. Matsui E, Kaneko H, Teramoto T, Fukao T, Inoue R, Kasahara K, Takemura M, Seishima M and Kondo N: Reduced IFN-gamma production in response to IL-12 stimulation and/or reduced IL-12 production in atopic patients. *Clin Exp Allergy* 30: 1250-1256, 2000.

17. Del Prete G, De Carli M, Almerigogna F, Giudizi MG, Biagiotti R and Romagnani S: Human IL-10 is produced by both type 1 helper (Th1) and type 2 helper (Th2) T cell clones and inhibits their antigen-specific proliferation and cytokine production. *J Immunol* 150: 353-360, 1993.
18. Wanidworanun C and Strober W: Predominant role of tumor necrosis factor-alpha in human monocyte IL-10 synthesis. *J Immunol* 151: 6853-6861, 1993.
19. Takanashi S, Nonaka R, Xing Z, O'Byrne P, Dolovich J and Jordana M: Interleukin 10 inhibits lipopolysaccharide-induced survival and cytokine production by human peripheral blood eosinophils. *J Exp Med* 180: 711-715, 1994.
20. Arock M, Zuany-Amorim C, Singer M, Benhamou M and Pretolani M: Interleukin 10 inhibits cytokine generation from mast cells. *Eur J Immunol* 26: 166-170, 1997.
21. Marshall JS, Leal-Berumen I, Nielsen L, Glibetic M and Jordana M: Interleukin (IL)-10 inhibits long-term IL-6 production but not preformed mediator release from rat peritoneal mast cells. *J Clin Invest* 97: 1122-1128, 1996.
22. Ding L, Linsley PS, Huang LY, Germain RN and Shevach EM: IL-10 inhibits macrophage costimulatory activity by selectively inhibiting the up-regulation of B7 expression. *J Immunol* 151: 1224-1234, 1993.
23. John M, Lim S, Seybold J, Jose P, Robichaud A, O'Connor B, Barnes PJ and Chung KF: Inhaled corticosteroids increase interleukin-10 but reduce macrophage inflammatory protein-1, granulocyte-macrophage colony-stimulating factor, and interferon-gamma release from alveolar macrophages in asthma. *Am J Respir Crit Care Med* 157: 256-262, 1998.
24. Borish L, Aarons A, Rumbly J, Cvietusa P, Negri J and Wenzel S: Interleukin-10 regulation in normal subjects and patients with asthma. *J Allergy Clin Immunol* 97: 1288-1296, 1996.
25. De Waal Malefyt R, Haanen J, Spits H, Roncarolo MG, Te Velde A, Figdor C, Johnson K, Kastelein R, Yssel H and De Vries JE: Interleukin 10 (IL-10) and viral IL-10 strongly reduce antigen-specific human T cell proliferation by diminishing the antigen-presenting capacity of monocytes via downregulation of class II major histocompatibility complex expression. *J Exp Med* 174: 915-924, 1991.
26. Schandene L, Alonso-Vega C, Willems F, Gerard C, Delvaux A, Velu T, Devos R, De Boer M and Goldman M: B7/CD28-dependent IL-5 production by human resting T cells is inhibited by IL-10. *J Immunol* 152: 4368-4374, 1994.
27. Sakaguchi S: Regulatory T cells: mediating compromises between host and parasite. *Nat Immunol* 4: 10-11, 2003.
28. Bellinghausen I, Klostermann B, Knop J and Saloga J: Human CD4⁺CD25⁺ T cells derived from the majority of atopic donors are able to suppress TH1 and TH2 cytokine production. *J Allergy Clin Immunol* 111: 862-868, 2003.
29. Wilson MS, Elnekave E, Mentink-Kane MM, Hodges MG, Pesce JT, Ramalingam TR, Thompson RW, Kamanaka M, Flavell RA, Keane-Myers A, Cheever AW and Wynn TA: IL-13 Ralpha2 and IL-10 coordinately suppress airway inflammation, airway-hyperreactivity, and fibrosis in mice. *J Clin Invest* 117: 2941-2951, 2007.